PRELIMINARY RESULTS OF TAT-MEDIATED PHOTOACTIVATABLE CELL DELIVERY

An Honors Fellows Thesis

by

MATTHEW ELLIS GRUNEWALD

Submitted to the Honors Programs Office
Texas A&M University
in partial fulfillment of the requirements for the designation as

HONORS UNDERGRADUATE RESEARCH FELLOW

April 2011

Major: Biochemistry
Genetics

PRELIMINARY RESULTS OF TAT-MEDIATED PHOTOACTIVATABLE CELL DELIVERY

An Honors Fellows Thesis

by

MATTHEW ELLIS GRUNEWALD

Submitted to the Honors Programs Office
Texas A&M University
in partial fulfillment of the requirements for the designation as

HONORS UNDERGRADUATE RESEARCH FELLOW

Approved by:

Research Advisor:	Jean-Philippe Pellois
Associate Director of the Honors Programs Office:	Dave A. Louis

April 2011

Major: Biochemistry
Genetics

ABSTRACT

Preliminary Results for TAT-Mediated Photoactivatable Cell Delivery. (April 2011)

Matthew Ellis Grunewald
Department of Biochemistry and Biophysics
Texas A&M University

Research Advisor: Dr. Jean-Philippe Pellois
Department of Biochemistry and Biophysics

Protein delivery into cells is often achieved through use of cell-penetrating peptides (CPPs). TAT (an HIV peptide) is one of the most efficient CPPs and, when incubated with cells, induces macropinocytosis of the surrounding medium. This brings coincubated extracellular cargo into endosomes, where they often remain trapped without outside stimulus. We hypothesized that TMR conjugated to TAT could induce medium uptake and, when photoactivated by light treatment, cause endosomal release of cargo. We performed several experiments using TMR-TAT and eGFP cargo at various conditions, but initial trials show no detectable delivery. Though our results are only preliminary, we have observed several phenomena that inhibit delivery and/or detection of delivery, including low endosomal uptake and release, fluorescent CPP adherence to the dish surface, and high cell death and buildup of cellular debris. In future trials, we plan to correct these issues by modifying reagent concentrations, using different reagents, and changing intensity of light treatment. In summary, we believe delivery is

still possible after changing various parameters. If future trials are successful, TMR-TAT and cargo coincubation may prove to be an efficient method to deliver therapeutic proteins and has implications in patient drug treatment and *in vitro* cell modulation.

ACKNOWLEDGMENTS

I would like to thank Dr. Jean-Philippe Pellois for his excellent mentoring and guidance and for his contribution on microinjection work. I thank Nandhini Muthukrishnan for her thorough training and for her work on delivery and peptide synthesis. I would like to acknowledge Ya-Jung Lee for her guidance and encouragement and Divyamani Srinivasan for her exceptional training. An activated reagent for peptide synthesis was created by Jongdoo Lim, and delivery peptides were synthesized by Alfredo Erazo-Oliveras. Grant money was provided by NIH. Finally, I thank the Honors Office and Dave Louis for encouragement, guidance, and the opportunity to present my results.

NOMENCLATURE

Cargo	The biomolecule to be delivered into the cell
CPP	Cell-penetrating peptide, facilitates cargo internalization into cells, e.g. TAT
Crocetin	Singlet oxygen scavenger, inhibits TMR-mediated endosomal release
eGFP	Enhanced green fluorescent protein, used as cargo
FITC	A green fluorophore, used as cargo or as photosensitizer
HA2	Influenza hemagglutinin, induces membrane leakage at low pH
PCI	Photochemical internalization, light-mediated delivery
PDT	Photodynamic therapy, method of photoinduced cell death
Photosensitizer	Photoexcitable chemical used to kill cells in PDT
PTD	Protein transduction domain, CPP part of a protein
ROI	Reactive oxygen species
Singlet oxygen	Unstable ROS, responsible for death in PDT
SYTOX Blue	Nuclear stain to detect cell death
TAT	HIV transactivator of transcription, CPP used in our studies

TABLE OF CONTENTS

LIST OF FIGURES

CHAPTER I

INTRODUCTION

Rationale

In general, delivery of exogenous or foreign compounds into cells or tissues is difficult. Oral ingestion and direct injection are historically the most common methods of drug delivery due to simplicity of administration. Unfortunately, these routes of delivery allow only a slim margin of possible drugs that balance properties need for effective transfer, including lipophilicity, lack of polarity, metabolic stability (1). Clearly new methods to deliver polar and hydrophilic biomolecules, such as proteins, needs to be pursued. Currently, one of the most studied forms of delivery is transduction of extracellular biomolecules across the plasma membrane into the cell.

Once a competent and reliable method of direct molecule transduction is developed, it will have applications in many biological and chemical areas. For instance, fluorescent markers (e.g. eGFP and derivatives, quantum dots, etc.) and metabolic markers could be transduced into culture or tissue cells to study localization and duration of biochemical processes in real time (2). Antibodies could be used for intracellular purposes, including neutralization of viral proteins, diagnosis of disorders, and specific biomolecule imaging

---

This thesis follows the style of *The Journal Biological Chemistry*.

(3). Protein/peptide-based therapeutic drugs, especially anticancer molecules, could be delivered directly to site of damage (4). Transcription factors and growth/differentiation factors could be applied *in vitro* or *in vivo* to direct cell fate or even induce pluripotency (5). Finally, nonprotein molecules such as MRI contrast agents and nucleic acids could be used to enhance magnetic imaging resolution and direct gene expression respectively (6).

Cell-penetrating peptides

The lipid bilayer membrane of eukaryotic cells has evolved into a tightly regulated barrier that controls biomolecule translocation. This membrane system has adapted well to keep unnecessary and possibly harmful components out of the cell. This poses a significant barrier to delivery of exogenous chemicals, especially proteins and other macromolecules. Mechanical and electrical methods to bypass this barrier often risk compromising membrane integrity and/or are very technical and time consuming (7). Transduction methods that exploit intrinsic biological processes have been proposed and studied, though most are inefficient and show inconsistent results. Several studies have shown the importance of cell-penetrating peptides (CPPs), which can be utilized in conjugation with the cargo molecule to effect delivery into a cell.

CPPs are a group of peptides that enhance cellular uptake of surrounding molecules by various means. In general, CPPs are usually short peptide sequences with several positively charged residues (usually lysine or arginine). A CPP could be isolated from

an organism, usually as a protein domain (or protein transduction domain/PTD), or be a synthetic construct, often to mimic a known PTD. Common PTDs include the TAT domain (from the HIV transactivator of transcription) and penetratin (the third α helix of Drosophila antennapedia homeodomain), and synthetic CPPs include R9 (arginine nonamer) and transportan (a chimeric peptide) (6).

TAT as a mediator of delivery

The TAT domain, simplified to TAT, is one of the most studied CPPs to date. The peptide is found naturally as a PTD of the TAT protein of HIV, which activates transcription of viral genes in the host cell nucleus. In 1988, Frankel *et al.* observed spontaneous cellular uptake of TAT protein (8). This ability to induce internalization is conserved in a small region (~10 amino acids, sequence: GRKKRRQRRRG) of the protein (9), which is typically the only region used for experimental transductions.

The mechanisms behind TAT-induced transduction are not fully understood but seem to be complex and involve several different methods of internalization. TAT directly crosses the plasma membrane into the cytosol at extracellular concentrations above a threshold (~10 μM) (10). Below this threshold, endocytic internalization pathways predominate, especially macropinocytosis (mass uptake of surrounding medium) (11). This uptake seems to be dependent on cell matrix heparin sulfate proteoglycans (12), and positively-charged TAT binds directly to the negatively-charged heparin sulfate

moieties, mediated by ionic interactions (13). After transduction, TAT localizes to the nucleoli of the cell nucleus (14).

Several methods have been studied to exploit TAT-mediated internalization for delivery of cargo molecules into cells. The simplest method is incubation of cells in medium containing TAT conjugated directly to the cargo of interest. But after the TAT-cargo is taken up by the cell, it often remains trapped in the endosomes and is eventually degraded by lysosomal fusion. A regulatable method to induce endosomal lysis must be introduced to release the cargo into the cytosol before it is degraded. For instance, the influenza hemagglutinin protein HA2 can be ligated to the TAT-cargo complex. HA2 promotes membrane fusion and leakage at low pH levels, initiating release of endosomal contents after slight acidification from endosomal maturation/lysosomal fusion (15). This improves delivery significantly but requires modification of the cargo, possibly altering its function or final destination (TAT localizes to the nucleoli.). Recently we showed that TAT conjugated to E5 (a HA2 derivative) coincubated with unmodified cargo is sufficient to induce endocytosis and cargo release into the cytosol (16). But this method still shows relatively low rates of delivery and is regulated by the pH of the endosomes—it cannot be manually controlled.

Photoacceleration of delivery

In recent decades, significant progress has been made in initiation/regulation of biochemical reactions by light treatment. Of note is the cytotoxic treatment called

photodynamic therapy, or PDT. PDT involves directly or intravenously treating cells, usually cancerous, with a photosensitizer, which is general inert in the absence of light treatment. Damaged or cancerous tissue is then irradiated by light of a specific wavelength, activating the photosensitizer. (An ideal photosensitizer is also selectively favored for absorption by cancerous cells.) Photoactivation initiates several biochemical reactions that interrupt cellular processes, killing the irradiated cells (17).

The mechanisms behind photoactivated cell death are complex and not fully understood. In general, photosensitizers are easily photoexcited to a higher electronic state. Energy from this excited state is transferred via several routes, including radiative (fluorescence) and nonradiative (heat) decay or direct electron transfer. This can lead to production of reactive oxygen species (ROS) by several different routes. For example, an excited photosensitizer can directly transfer an electron to O_2, eventually leading to formation of H_2O_2 (18). H_2O_2 can then diffuse throughout the cell and split into reactive hydroxyl radicals, which can react with nearly any biomolecule (19). Most PDT protocols use a chemical with high singlet oxygen ($^1O_2$) production capability, such as porphyrin-like molecules (20). Singlet oxygen is a ROS with a highly unstable spin state configuration that is formed from direct energy transfer from the excited photosensitizer (21). Due to its instability, singlet oxygen possesses a very short lifetime, and its area of reactivity is limited to the immediate area around the photosensitizer (18). Even so, $^1O_2$ formation is one of the primary mechanisms driving PDT-induced cell process disruption and death.

We recently showed that induction of cell death was possible via singlet oxygen production by photosensitized TMR (tetramethylrhodamine), even this fluorophore possesses low $^1O_2$ production ability. TMR by itself is incapable of membrane lysis and is nontoxic to cells, even in the presence of significant light. However, when conjugated to TAT, TMR-TAT is lethal during photosensitization after incubation (22). We proposed the following model: TMR-TAT is internalized into endosomes, and membrane-associated TAT localizes TMR to inner face of the endosome. Light treatment electronically excites TMR, causing singlet oxygen production and endosomal leakage. TMR-TAT then escapes into the cytosol, allowing disruption of the plasma membrane and cell death (22).

The PDT protocol can be modified to deliver biomolecules, allowing manual temporal and spatial control. This method is called photochemical internalization (PCI) and uses light as a mediator of endosomal cargo release. In order to prevent cell death seen in PDT, PCI utilizes less reactive photosensitizers such as TMR or fluorescein (FITC) in conjunction with a CPP such as TAT. Matsushita *et al*. showed light treatment induces endosomal release and cytosolic delivery of 11R-p53 (polyarginine CPP ligated to p53, an anticancer protein) conjugated to the fluorophore FITC after internalization (23). Finally, Gillmeister *et al*. showed that TMR-labeled TAT-GFP can be delivered by similar internalization and light treatment (24). But both these experiments require modification of the cargo (p53 or GFP), possibly altering cargo function or

localization. Furthermore, the reactive photosensitizer is conjugated directly to the cargo, which could result in chemical alterations.

Our method

In the experiments presented here, we tested a novel method of photochemical internalization mediated by TMR-TAT. We coincubated HeLa cells with TMR-TAT and unmodified eGFP to induce cellular uptake of both. We then visualized the resulting localization patterns of both fluorophores and attempted to photoaccelerate TMR-TAT-mediated endosomal release by light treatment at various intensities. Presumably, we can prevent continued membrane lysis by varying light treatment parameters.

Furthermore, we hypothesized that cytotoxicity associated with photoactivation of fluorescent CPP can be mitigated by replacing TMR-TAT with TMR conjugated to TAT by a disulfide bond (TMR-SS-TAT). We have previously shown that biomolecules delivered into the cytosol will be cleaved at any exposed disulfide bond (2). This break is caused by interaction with free glutathione (25), a cytosolic tripeptide composed of glycine, cysteine, and glutamic acid and involved in protein function and degradation of xenobiotics (e.g. drugs) (26). Assumedly, after endosomal release, glutathione will cleave TMR-SS-TAT into nontoxic TMR and TAT, preventing localization of activated TMR to the plasma membrane and preventing lysis. This hypothesis is based on our current model of TMR-TAT-induced cell death (22), and using TMR-SS-TAT should allow equivalent delivery with less chance of initiating apoptosis.

CHAPTER II

METHODS

Reagents

Synthesis of TMR-TAT

TAT peptide was synthesized by Fmoc solid-phase peptide synthesis using a rink amide MBHA resin substrate as described previously (2). In short, Fmoc protected N-terminus amino acids were activated by HBTU, added to the resin, and deprotected by piperidine. The process was repeated until the TAT peptide (sequence: GRKKRRQRRRG) was completed. TAMRA (5- (and 6-) carboxytetramethylrhodamine) was added to the N-terminus of the peptide, forming TMR-TAT. Product was removed from the resin by TFA and purified by HPLC.

Fmoc (D)-amino acids and TMR were purchased from Novabiochem, and all other chemical reagents were purchased from Sigma-Aldrich.

Synthesis of TMR-SS-TAT

TAMRA ligated to pyridyldithio-ethylamine via the 5,6 carboxylic acid group was given to us by the lab of Jongdoo Lim. Cysteine-TAT (sequence: CGRKKRRQRRRG) was synthesized by solid phase peptide synthesis as described above. Cys-TAT was reacted with the disulfide-activated TMR in Tris-Cl for 3 hours. Product was purified by HPLC.

Synthesis of eGFP

pTXB1-eGFP plasmid was transformed into BL21 *E. coli* bacteria (Thermo Fisher) and cultured in 6 liters LB medium (Thermo Fisher) at 37° C. At mid-log growth phase (OD_{600} = 0.6), bacteria were induced with 0.5 mM IPTG (Thermo Fisher) and cultured for 4 hours at 37° C. Cells were pelleted, resuspended in lysis buffer (20 mM Tris-Cl, 200 mM NaCl), and sonicated (3000 Sonicator, Misonix Inc.). After lysate fractionation by centrifuge (14,000 RPM for 40 min at 4° C), the soluble fraction was added to chitin beads (New England Biolabs) in lysis buffer and incubated at 4° C for 24 hours. (Proteins bind to the beads via the C-terminal intein-chitin binding domain/CBD purification tag.)

The bead mixture was washed several times in a column with lysis buffer to remove unbound proteins. Beads were then incubated for 24 hours in cleavage buffer (100 mM HEPES, 200 mM NaCl, 100 mM MESNA) to induce cleavage of eGFP-intein CBD from the intein-CBD-bead complexes. Free eGFP was collected by several cleavage buffer washes and purified through an ion exchange column. Samples were concentrated by Centricon spin filtration (Millipore), confirmed by mass spectroscopy, and quantified by absorbance ($\varepsilon_{488\ nm}$ = 55,000 $M^{-1}cm^{-1}$) (27).

All chemical reagents were purchased from Sigma Aldrich.

Assay specifications

Cell lines

The HeLa cervical cancer cell line was used in all experiments. Cells were cultured in DMEM with 10% FBS in a 10 cm dish kept in a 5% CO_2 incubator at 37° C. Cells were passaged every 2-3 days when above 80% confluency. Passaging protocol included removal of media, washes with PBS, incubation with 0.5% trypsin, 4-10x dilution by with DMEM, and inoculation onto a second dish.

DMEM, FBS, trypsin EDTA, and PBS were purchased from Thermo Fisher, and Corning dishes were purchased from Sigma Aldrich.

Delivery specifications

Cells were subcultured in an 8-well dish overnight until 60-80% confluency. Media was removed, and cells were washed three times with either PBS or L-15 medium. Medium containing 1-2 μM CPP and/or 10-20 μM eGFP either with or without 50 μM crocetin (a inhibitor of photosensitization) was added, and cells were incubated at 37° C in the dark for 1 hour. Cells were washed three times again with PBS or L-15 and kept at 37° C in cysteine-free L-15 either with or without 5 μM SYTOX Blue DNA stain for visualization and light treatment.

8-well dishes were purchased from Thermo Fisher, crocetin was purchased from Sigma Aldrich, and Leibovitz L-15 and SYTOX Blue were purchased from Invitrogen.

Microinjection

HeLa cells were plated on 35 mm plates (P35G-1.5-7-C-grid, MatTek Corp.) at ~100,000 cells/mL in 2 mL DMEM and later washed and incubated with L-15. 10 μM TMR-TAT was mixed with 10 μM 70 kDa Dextran-fluorescein, and femtoliter aliquots were directly injected into the cytoplasm of live HeLa cells using a FemtoJet microinjector controlled by an InjectMan NI2 micromanipulator (Eppendorf). Microinjected cells were imaged/photoactivated, and cytosolic microinjection was confirmed by observing nuclear exclusion of 70 kDa Dextran.

Fluorescent microscopy

Cells were observed with a fluorescence inverted microscope with a spinning disk for confocal and wide-field visualization (microscope model: IX81 from Olympus). The microscope was mounted with a 37° C stage for cell incubation and fitted with a back-illuminated EMCCD chip camera (model: Rolera-MGI Plus from Qimaging) for imaging. Samples were visualized by bright field imaging and with fluorescent light from a 100 W halogen lamp with RFP (λ_{ex} = 560±20 nm; λ_{em} = 630±35 nm), FITC (λ_{ex} = 482±35 nm; λ_{em} = 536±40 nm), and CFP (λ_{ex} = 436±20 nm; λ_{em} = 480±40 nm) standard fluorescent filter sets. The RFP filter was used for photoactivation of fluorescent CPP and was controlled manually by varying neutral density filters (100%, 25%, 12.5%, or 5% transmittance) and exposure time. Olympus SlideBook 4.2 software was used for fluorescence intensity quantification and image modulation (e.g. deconvolution, contrast modification, etc.).

CHAPTER III

RESULTS

We performed several trials of cargo/CPP coincubation in HeLa cells with the goal of endosomal release and cargo delivery. TMR-TAT or TMR-SS-TAT served as CPPs with eGFP as cargo. After incubation and washing, cells were visualized by confocal microscopy and photoactivated by the RFP fluorescence filter. To date, no trials have shown effective/quantifiable delivery of cargo eGFP. It is important to note that these are only preliminary results, and few trials were sufficiently repeated. But if our trial results are reliable, trends and general phenomena inhibiting delivery can be observed in these preliminary trials.

Cargo and CPP show endosomal localization but inefficient delivery

CPP and cargo visualization with respective fluorescent filters (RFP and FITC) showed punctate (spotted) distribution, indicating endosomal localization of both fluorophores. **Figure 1** shows standard images of each. It was difficult to view cells with both filters in one image due to major differences in measured intensities of green and red fluorescence. Visualization of green vesicles could only be accomplished with higher fluorescent intensities (100-50% transmittance). Under these conditions, red fluorescence was too intense and was quickly photobleached (lost fluorescence due to fluorophore decay). This disparity in observed intensities is partly a result of differences in UV light source intensities between the two filters. Even so, because fluorescent

intensities of visible endosomes measured only slightly above background levels, both CPP and cargo displayed low endosomal uptake.

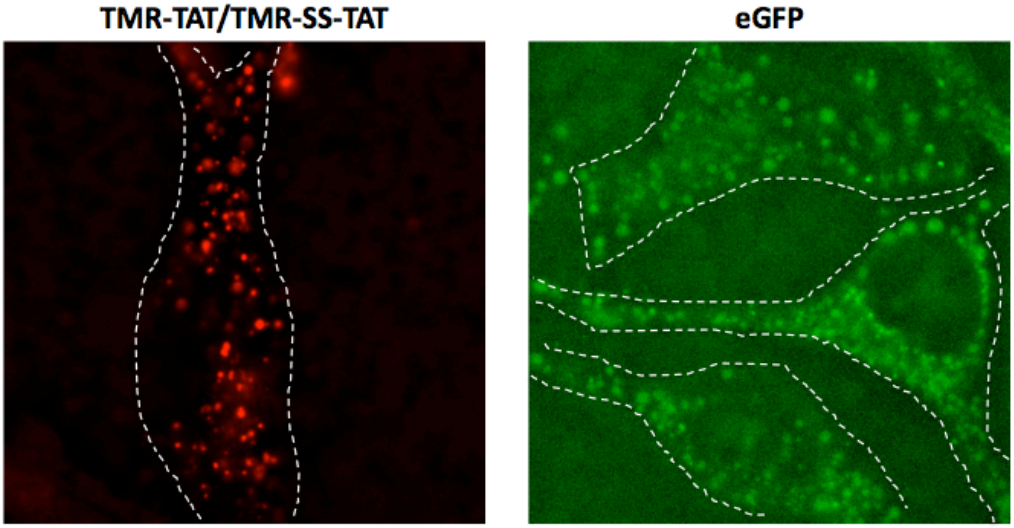

FIGURE 1. **Endosomal Localization of CPP and Cargo**. Before photoactivation, both CPP and cargo show punctate distribution indicative of endosomes. RFP filter fluorescence is higher than FITC, which is due, in part, to detection priority of the microscope. Both images are deconvoluted, and cell outlines are traced.

After we confirmed evidence of punctated endosomal fluorescence, we attempted to induce endosomolysis by fluorescent CPP photoacceleration using RFP filter light pulses at various intensities and exposure times. Successful delivery was defined by loss of punctate distribution coupled with increasing diffused (cytosolic) fluorescence at most points outside the nucleus. Using these criteria as standards, we were unable to induce any discernable release of cargo or CPP into the cytosol. Most trials were unsuccessful due solely to the inability to visualize cells properly—reagent-dish interactions and cellular debris (described later) often inhibited proper contrast between background and endosomal fluorescence. For the few trials that produced qualifiable images, fluorescent

distribution remained punctate, accompanied with red and green photobleaching and cell death. TMR-TAT and TMR-SS-TAT showed no difference in fluorescence or functionality.

TMR-TAT photoactivation results in cell death even without significant endosomal release

CPP coincubated with cargo failed to induce CPP release, contradicting previously observed results from PDT experiments that used TMR-TAT to induce apoptosis (22). This may be due to CPP-cargo interactions that inhibit proper endosomolysis. Even cells incubated for 15 minutes with only eGFP and visualized with FITC showed noticeable death rates (data not shown), so the effect may be cumulative. We incubated cells with TMR-TAT alone to attempt to reproduce previous results from our PDT trials. Interestingly, we could not induce detectable release of TMR-TAT into the cytosol but still observed consistent cell death after every pulse. **Figure 2** shows the results of one pulse trial, and **Supplementary Video 1** shows time-lapse imaging of a continuous RFP pulse with no visible endosomal release. It is possible that endosomal release was occurring at a low level but was masked by photobleaching and loss of overall fluorescence. Furthermore, it should be noted that this was only one trial and may be anomalous. We plan to replicate the conditions to confirm our preliminary findings.

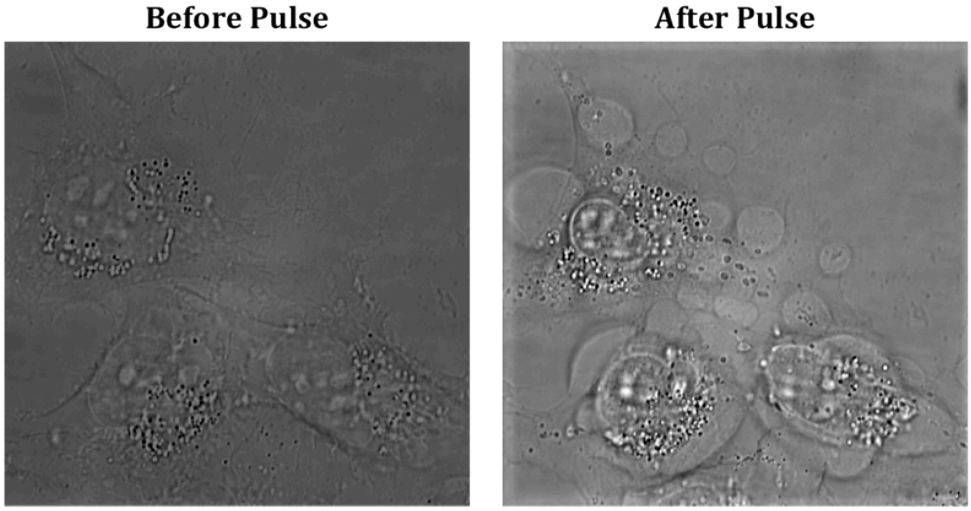

FIGURE 2. **Effects of Light Toxicity of TMR-TAT**. Healthy cells were exposed to an RFP filter high intensity (100-50%) pulse for 10 sec. Cells died by apoptosis quickly, as evidenced by membrane protrusion, rounding morphology, and weakened nuclear integrity.

Photoactivated TMR-TAT microinjected directly into cells does not induce death

To determine if activated TMR-TAT that had escaped endosomes, even at undetectable levels, is responsible for cell death, we microinjected TMR-TAT directly into HeLa cells and treated with light under various conditions. We hypothesized that TAT should localize to the inner face of the cytosolic membrane and, upon photoactivation, lyse the membrane, analogous to the proposed mechanism of cell death from TMR-TAT endosomolysis (22). All trials except one showed no cell death despite several minutes of RFP exposure. Cells visibly took up TMR-TAT and displayed significant fluorescence but showed no noticeable change in morphology, nuclear structure, or outer membrane stability (standard indicators of cell death). **Supplementary Video 2** shows a representative time-lapse of single trial.

The disulfide bond of TMR-SS-TAT does not prevent cell death

To decrease the cytoxicity of TMR-TAT, we ligated TMR to TAT via a disulfide bond. This bond should be reduced by glutathione in the cytosol after endosomal escape, which prevent TAT from localizing TMR to the membrane (25). After we coincubated and washed cells, we added SYTOX Blue, a dye that stains the nucleus upon cell death. We examined cells using the CFP fluorescent filter before and after an RFP pulse at various intensities and exposure times. Preliminary tests show that the disulfide bond does not reduce cytoxicity, and most treated cells died after the pulse. Even when cells were incubated and photoactivated in the presence of crocetin, a singlet oxygen inhibitor that we previously showed inhibited TMR-TAT-induced cell death (22), apoptosis still occurred. **Figure 3** shows an example trial with a 2.5 min pulse at the lowest intensity (5%). We are currently undergoing cell viability trials testing only TMR-SS-TAT without cargo to better quantify our initial findings.

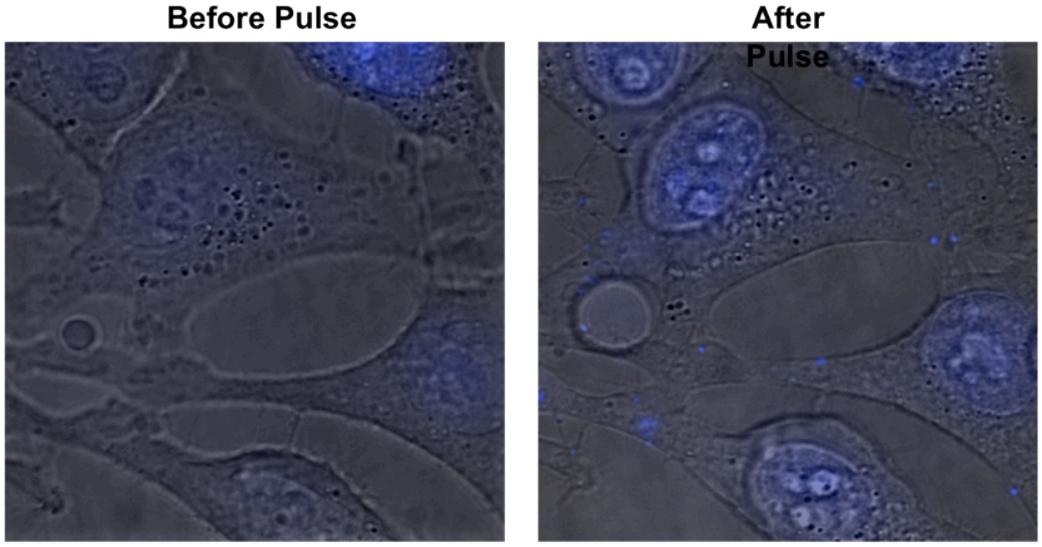

FIGURE 3. **SYTOX Blue Test to Detect TMR-SS-TAT-Induced Cell Death**. Cells were incubated with TMR-SS-TAT, eGFP, SYTOX Blue, and singlet O_2 inhibitor crocetin. Before the RFP pulse, only one cell (upper right) was dead, as shown by the distinct, blue-stained nucleus. After a 2.5 min RFP pulse, all cells had died and showed prominent nuclei with permeability to SYTOX Blue.

Reagent incubation results in cell death and cellular debris

As we prepared each experiment, we observed general cell morphology and confluency before and after each wash and incubation. First wash triplicates reduced cell confluency, usually by 10%-20%. We also observed significant dark toxicity (cell death without photoactivation) when cells were incubated with a CPP—after the second set of washes, confluency was reduced to 10%-20%, and we observed several patches of dead cells (**Figure 4**). The cause of this toxicity without photosensitization is unknown.

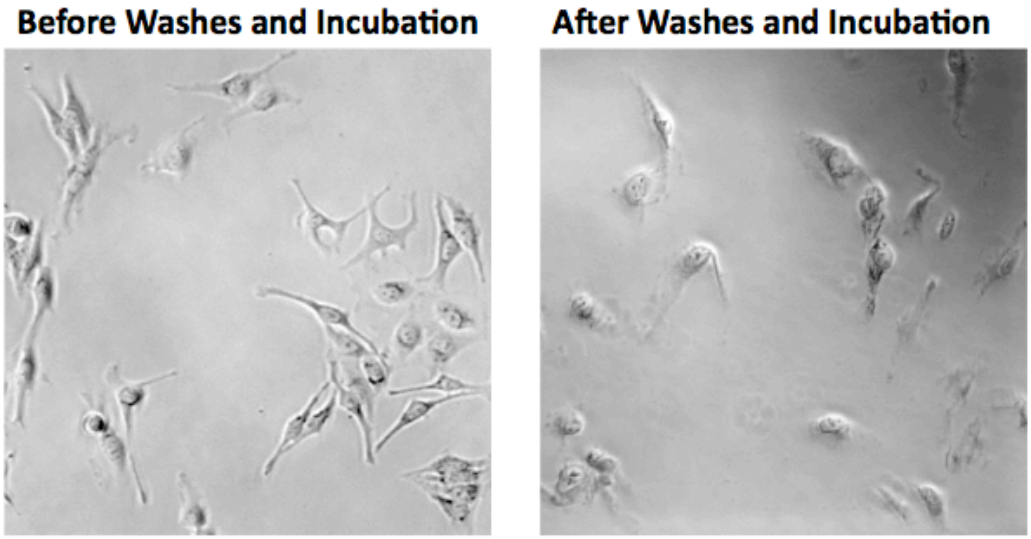

FIGURE 4. **Effects of Dark Toxicity**. After overnight incubation, cells were at 50%-80% confluency and showed negligible death rates. After incubation with CPP and cargo, cells were reduced to 10%-20% confluency and showed low viability, as evidenced by rounded morphology and raised nuclei.

Furthermore, as cells continued to die, cellular debris began to accumulate and float throughout the dish. These clusters seemed to be stained by eGFP cargo and were highly fluorescent when viewed under the FITC filter (**Figure 5**). This high fluorescence inhibited proper visualization of less fluorescent cargo in the endosomes and prevented delivery verification for many trials. Most debris appeared after the second set of washes, possibly associating with eGFP during the 1 hour incubation, and continued to increase during visualization. Therefore, this debris seems to be a direct result of cell apoptosis and fragmentation.

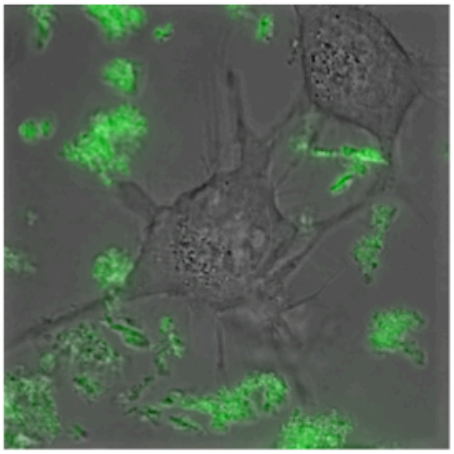

FIGURE 5. **Fluorescence of Cellular Debris**. Debris accumulates as cells die. The fragments interact with the cargo fluorophore, skewing the contrast of the image, and preventing proper visualization of endosomal cargo.

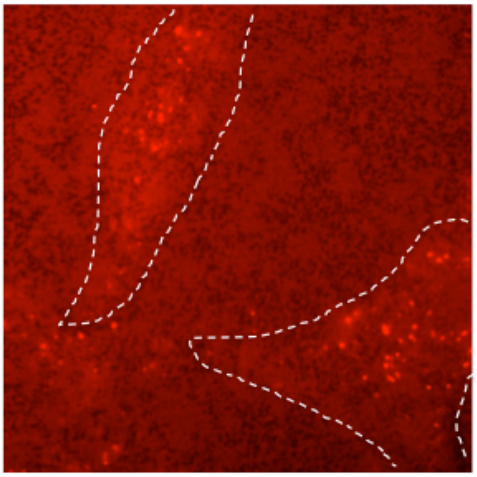

FIGURE 6. **Interference by CPP Adherence to Dish**. In all trials, TMR-SS-TAT (shown here) or TMR-TAT adhered to the top of the dish, creating a speckled pattern. The attached CPP creates higher background fluorescence, lessening contrast with vesicular TMR-TAT (top middle and bottom right).

Both fluorescent CPPs stick to dish surface

Throughout all trials, we observed significant background fluorescence from the dish itself. Upon observation, we noticed a speckled pattern that seemed to be a result from fluorescent CPP (either TMR-TAT or TMR-SS-TAT) sticking to the surface of the well. We confirmed that this signal was a result of incubation with CPP by comparison with background signal from an untreated dish (**Figure A.1**). The speckled background fluorescence was not overwhelmingly high but still interfered with endosomal visualization by lowering the contrast ratio (**Figure 6**). Because endosomal fluorescence was low, this effectively prevented confirmation of release for several trials.

Furthermore, it is possible that residual CPP on the dish surface could interact with different cellular processes and structures in the HeLa cells themselves.

CHAPTER IV

ANALYSIS OF FINDINGS

While our initial trials were unsuccessful, we were able to observe and characterize several issues that directly or indirectly inhibit proper delivery of eGFP. Low endosomal concentration and release, CPP-dish adherence, and abnormally high cell death rates posed the biggest obstacles to successful trials.

Possible causes of low endosomal uptake/release

Even for the trials that we could visualize properly (no/low cellular debris, etc.), we still were unable to detect delivery of TMR-TAT/TMR-SS-TAT or eGFP and saw low endosomal uptake and low release. These two processes of delivery are directly related—low uptake levels lead to low release. It is reasonable to assume that some threshold level of activated TMR positioned near the endosomal membrane by TAT is required for proper $^1O_2$ production and membrane lysis/leakage. If fluorescent CPP concentrated in the endosome is unable to surpass this microenvironment threshold, release may not occur at a detectable level.

Low uptake and release in trials with TMR-SS-TAT could possibly be due to spontaneous reduction and cleavage of the disulfide bond. This would inhibit TAT-mediated concentration of the fluorophore into the endosome and also prevent endosomolysis. TAT could no longer localize TMR to the endosomal membrane,

rendering light treatment ineffective. (We have previously shown that simple coincubation of unbound TMR and TAT fails to induce endosomolysis and death (22)). This disulfide cleavage may be a result of an external reducing agent in the media (e.g. cysteine) or a cellular metabolite, either secreted or endosomal.

For both fluorescent CPPs, low uptake levels could be a result of cargo interference that impairs TAT interaction with cell surface heparin sulfate proteoglycans to induce proper macropinocytosis. Similar or different interactions could occur in the endosome, preventing proper orientation of TMR for membrane lysis. These interactions could be complex and may be a result of many different submolecular interactions. Past experiments by others have shown that protein delivery is cargo-dependent to some extent (28).

Because we could not induce endosomolysis when HeLa cells were incubated with TMR-TAT alone (**Supplementary Video 1**), CPP-cargo interactions cannot be the only factor inhibiting release. Inability to release TMR-TAT from endosomes is a direct contradiction to previous trials which showed dispersal of TMR-TAT immediately before apoptosis (22). This implies that the causes behind low TMR-TAT (and TMR-SS-TAT) release may simply be due to use of inactive/damaged reagents. We have noticed that synthesis/processing of our photosensitive reagents (TMR-TAT/TMR-SS-TAT) under ambient light reduces functionality and fluorescence, presumably due to photobleaching. Our TMR-TAT stock solution could have been inactivated by transport

during synthesis. We have instituted new methods of peptide synthesis and now keep most reagents in a dark environment to preserve photoactivity. Further trials with new stock solutions are needed to test this theory.

Finally, this inability to induce release in the PDT replication experiment (incubation with TMR-TAT alone) could have been anomalous. We were only able to perform one set of trials, and any number to environmental factors (sick cells, bad media, etc) could have conceivably interfered with proper delivery. Surprisingly, we were able to induce apoptosis with all pulses (**Figure 2**), indicating that some biomolecular cell process catalyzed by light treatment was occurring. Repeats of TMR-TAT controls are needed to further support these initial findings.

Effects of fluorescent CPP-dish interaction

TMR-TAT/TMR-SS-TAT adherence to the dish is not an entirely new phenomenon—we have witnessed some degree of dish surface adherence in previous trials with many reagents. Some basal level of reagent loss always occurs, mostly at negligible quantities. But because uptake was low, the contrast between intra- and extracellular fluorescence is less, lowering the reliability of imaging (**Figure 6).** Furthermore, activated fluorescent CPP adhering to the dish may explain some cell death seen in all trials (explained below).

It is unknown whether the CPP is adhering directly to the dish or to some biomolecular intermediate. Elucidating these mechanisms could help to provide inhibitory methods to reduce this adherence.

Possible causes of cell death

Both TMR-TAT and TMR-SS-TAT displayed dark and light cytotoxicity (during incubation and visualization). We have often observed some degree of dark toxicity during incubation with other potential reactive reagents, including TAT-E5 (16). Normally, death during incubation is negligible and should be considered an unavoidable aspect of cell delivery. It is unexpected that our estimated death rates were so high (up to 60% confluency loss to death – **Figure 4**), even when incubated with normally innocuous eGFP. The cause of this toxicity is unknown, but such high rates may be cause for investigation.

We previously postulated that the cell death seen from TMR-TAT activation is due to reactive TMR escaping endosomes and disrupting the plasma membrane (22). Our observations from current trials have pushed us to reconsider this hypothesis. If cell death occurs primarily by loss of plasma membrane integrity, photoactivation of microinjected TMR-TAT should also induce cell death. Our results show that microinjected cells are resistant to light toxicity (**Supplementary Video 2**), implying that TMR-TAT-directed membrane instability may only be a minor factor in the cell death observed in our trials.

Other factors that drive cell death undoubtedly contribute, as evidenced by induction of cell death without endosomal release (**Supplementary Video 1**). In our previous model, TMR-TAT must diffuse through the cytosol to directly interact with the plasma membrane to cause death, which is impossible without endosomolysis. Furthermore, TMR-SS-TAT showed light toxicity, even though the disulfide motif has been shown to be cleaved in the reducing cytosol (2). Without this bond, TAT is incapable of localizing TMR to the cell membrane to induce lysis. Other mechanisms must be operating to explain these results.

It is possible that some undetectable release is occurring, allowing a small amount of TMR-TAT to escape and destroy the plasma membrane, requiring only a slight modification to our previous model. If only a minute concentration of TMR-TAT is needed for death, this could explain light toxicity associated with TMR-SS-TAT (**Figure 3**). A small portion of the CPP could escape disulfide reduction and, if above a minimum threshold, could disrupt other membrane structures. This modified model does not explain our microinjection results unless high intracellular concentrations of TMR-TAT are somehow inhibitory to cell death.

It is also possible that some TMR-produced reactive oxygen species, such as H_2O_2 or $^1O_2$, is able to diffuse to other areas of the cell and interfere with structural or metabolic functions. This proposed mechanism is compatible with other models and with all of our own experiments, except microinjection. Unfortunately, $^1O_2$ has a very short lifetime

(less than 1 μs), which impairs broad travel through the cell (18). $^1O_2$ would have to be localized in some manner by TMR near a disruptable biochemical structure. Finally, if non-$^1O_2$ ROS, such as H_2O_2, played a significant role in cell death, microinjected TMR-TAT would induce apoptosis. Because we could not produce this result, our previous model of death primarily by $^1O_2$ is supported.

Our inability to induce death from microinjection implicates that endosomal release is a integral step in fluorescent CPP-induced cell death. Late endosomes and lysosomes contain potentially toxic biomolecules, such as ROS and non-specific proteases that are destructive to the cell if released. Our dark incubation (1 hour) could allow unperturbed endosomal maturation, concentrating these toxic components in the endosome. Light treatment could incite release of these degradative chemicals and proteins, causing catastrophic loss of cellular homeostasis. No trials directly contradict this model, though apoptosis without endosomal release cannot be supported by this model alone. Again, it is possible that undetectable release occurred or that some other mechanism was contributing.

Finally, the cell membrane could be interacting with TMR-TAT adhering to the dish surface from incubation (**Figure 6**). During light treatment, this layer could be activated, causing lysis of the plasma membrane directly. This model is compatible with our previous experiments (22) and may show a cumulative effect with any other mechanism. Unfortunately, if this were true, microinjection should also induce death. It

is clear that photoinduced cell death is a complex and multifactorial phenomenon and requires further study.

CHAPTER V

FUTURE PLANS

Changes to current protocol

Varying reagent concentration

For our preliminary experiments, we used concentrations of CPP and cargo that have been optimized from previous tests (16,22). The next and simplest step would be to vary these concentrations to favor delivery instead of PDT. This includes decreasing the concentration of fluorescent CPP, which might reduce cell death and reagent adhesion to the dish. We could also increase the concentration of cargo, which would increase signal but could potentially increase cytotoxicity.

Crocetin in the medium during incubation and visualization did not prevent cell death (**Figure 3**). But because our trials were qualitative only, it could still theoretically have other effects, such as slowing the apoptotic process. Quantitative trials are needed, and increasing crocetin concentration could significantly reduce death. Finally, if death occurs due to catastrophic release of endosomal contents, the surrounding medium may need to be modified to compensate for released cytotoxic components. Possibilities include decreasing medium ion concentration and/or supplementation of protease or reactive oxygen species inhibitors.

Modifying the dish surfaces

Because reagent-dish interactions limit visualization and may influence cell death, it is worthwhile to limit residual TMR-TAT after washes. This can be accomplished by altering the reactivity of the dish surface by chemical or physical means. The simplest method is coating the dish with a reactive chemical substrate such as polylysine. In theory, the positive charges of lysine could repel highly cationic TAT, preventing adhesion. Furthermore, dishes coated with polylysine show higher cell adhesion (29), which may reduce loss of cells due to the mechanical stress of washing.

Varying exposure time and intensity

Photochemical internalization offers an advantage over other delivery methods by allowing manual control over the duration of endosomolysis by manipulating light treatment. While we have varied the intensity and time of our RFP pulse, we have not been able to prevent cell death. Therefore, fine-tuning the RFP pulse would probably optimize delivery once other aspects are under control but is not a determining factor of cell death. For example, if we can initiate predictable endosomal release, our next steps would be to quantify the duration of this release and correlate this duration to pulse parameters. Finally, once we limit cell death by changing other aspects of our protocol, we can relate pulse parameters to cell death rates to determine best conditions to balance delivery with death.

Using different reagents

While TMR may be useful as a low $^1O_2$-producing agent for PDT, it could be too cytotoxic for delivery at any concentration. We are currently investigating other agents that produce singlet oxygen or other reactive oxygen species. These new reagents may be more endosomolytic but less cytotoxic, or they may be less reactive to light, allowing finer control over release. Previous trials have proven that protein delivery efficiency is highly dependent on the cargo itself. Therefore, using a different cargo could more compatible with our TMR-TAT delivery protocol. Fluorescent dextrans may be ideal candidates due to nonreactivity and variability in size. We could also provide buffer-like components to balance out any undesired cargo side reactions. These could include emulsifiers to coat the cargo or counterions to neutralize charges. Though our initial tests showed that crocetin was unable to prevent eventual cell death, other oxygen scavengers could be better suited for our trials. Systematically using chemical inhibitors with different biochemical targets could also help to elucidate the mechanisms driving cell death.

Using different assays for delivery

So far, we have only used fluorescence as verification of delivery due to ease of use and ability to study delivery in real time. But recent problems inherent with our fluorescent trials (e.g. TMR-TAT adherence to dish, fluorescent cellular debris) prove that other assay methods need to be considered. Methods to assay functionality of a translocated biomolecule can also be utilized to determine delivery efficacy. For instance,

transducing mitogens (cell mitosis stimulants) and quantifying cell population, transducing transcription factors and quantifying expression, or transducing growth signals and quantifying cell differentiation are all possibilities. Such trials could also support the use of our TMR-TAT delivery method for modification of complex cellular processes or even for *in vivo* applications.

CHAPTER VI

SUMMARY AND CONCLUSIONS

In summary, though preliminary trials have been unsuccessful, we have been able to identify and study several obstacles that inhibit proper delivery. We show that inefficient uptake and release, reagent/dish interactions, and cell death all interact to prevent proper confirmation of delivery. We have been able to outline several modifications to our protocol to enhance the probability of success. Such modifications are minor, and we believe that delivery is still likely. If our trials are successful, we believe our TMR-TAT delivery method could have significant applications in a broad range of areas.

REFERENCES

1. Lipinski, C., and Hopkins, A. (2004) *Nature* **432**, 855-861

2. Lee, Y. J., Datta, S., and Pellois, J. P. (2008) *J Am Chem Soc* **130**, 2398-2399

3. Cornelissen, B., Hu, M., McLarty, K., Costantini, D., and Reilly, R. M. (2007) *Nucl Med Biol* **34**, 37-46

4. Wadia, J. S., and Dowdy, S. F. (2005) *Adv Drug Deliv Rev* **57**, 579-596

5. Kim, D., Kim, C. H., Moon, J. I., Chung, Y. G., Chang, M. Y., Han, B. S., Ko, S., Yang, E., Cha, K. Y., Lanza, R., and Kim, K. S. (2009) *Cell Stem Cell* **4**, 472-476

6. Stewart, K. M., Horton, K. L., and Kelley, S. O. (2008) *Org Biomol Chem* **6**, 2242-2255

7. Luo, D., and Saltzman, W. M. (2000) *Nat Biotechnol* **18**, 33-37

8. Frankel, A. D., and Pabo, C. O. (1988) *Cell* **55**, 1189-1193

9. Vives, E., Brodin, P., and Lebleu, B. (1997) *J Biol Chem* **272**, 16010-16017

10. Duchardt, F., Fotin-Mleczek, M., Schwarz, H., Fischer, R., and Brock, R. (2007) *Traffic* **8**, 848-866

11. Wadia, J. S., Stan, R. V., and Dowdy, S. F. (2004) *Nat Med* **10**, 310-315

12. Tyagi, M., Rusnati, M., Presta, M., and Giacca, M. (2001) *J Biol Chem* **276**, 3254-3261

13. Hakansson, S., Jacobs, A., and Caffrey, M. (2001) *Protein Sci* **10**, 2138-2139

14. Tunnemann, G., Martin, R. M., Haupt, S., Patsch, C., Edenhofer, F., and Cardoso, M. C. (2006) *FASEB J* **20**, 1775-1784

15. Wharton, S. A., Skehel, J. J., and Wiley, D. C. (1986) *Virology* **149**, 27-35

16. Lee, Y. J., Erazo-Oliveras, A., and Pellois, J. P. (2010) *Chembiochem* **11**, 325-330

17. Dolmans, D. E., Fukumura, D., and Jain, R. K. (2003) *Nat Rev Cancer* **3**, 380-387

18. Plaetzer, K., Krammer, B., Berlanda, J., Berr, F., and Kiesslich, T. (2009) *Lasers Med Sci* **24**, 259-268

19. Bergamini, C. M., Gambetti, S., Dondi, A., and Cervellati, C. (2004) *Curr Pharm Des* **10**, 1611-1626

20. Dougherty, T. J., Gomer, C. J., Henderson, B. W., Jori, G., Kessel, D., Korbelik, M., Moan, J., and Peng, Q. (1998) *J Natl Cancer Inst* **90**, 889-905

21. Karotki, A., Kruk, M., Drobizhev, M., Rebane, A., Nickel, E., and Spangler, C. W. (2001) *JSTQE* **7**, 971-975

22. Srinivasan, D., Muthukrishnan, N., Johnson, G. A., Erazo-Oliveras, A., Lim, J., Simanek, E. E., and Pellois, J. P. (2011) *PLoS One* **6**, e17732

23. Matsushita, M., Noguchi, H., Lu, Y. F., Tomizawa, K., Michiue, H., Li, S. T., Hirose, K., Bonner-Weir, S., and Matsui, H. (2004) *FEBS Lett* **572**, 221-226

24. Gillmeister, M. P., Betenbaugh, M. J., and Fishman, P. S. (2011) *Bioconjug Chem*

25. Hallbrink, M., Floren, A., Elmquist, A., Pooga, M., Bartfai, T., and Langel, U. (2001) *Biochim Biophys Acta* **1515**, 101-109

26. Pompella, A., Visvikis, A., Paolicchi, A., De Tata, V., and Casini, A. F. (2003) *Biochem Pharmacol* **66**, 1499-1503

27. McRae, S. R., Brown, C. L., and Bushell, G. R. (2005) *Protein Expr Purif* **41**, 121-127

28. El-Andaloussi, S., Jarver, P., Johansson, H. J., and Langel, U. (2007) *Biochem J* **407**, 285-292

29. Yavin, E., and Yavin, Z. (1974) *J Cell Biol* **62**, 540-546

APPENDIX I

TECHNICAL ACRONYMNS

CFP	Cyan fluorescent protein
DMEM	Dulbecco's modified eagle medium
FBS	Fetal bovine serum
FITC	Fluorescein isothiocyanate
HBTU	2-(1H-benzotriazol-1-yl)-1,1,3,3,-tetramethyluronium hexafluorophosphate
HEPES	4-(2-hydroxyethyl)-1-piperazineethanesulfonic acid
HPLC	High performance liquid chromatography
IPTG	Isopropyl β-D-1-thiogalactopyranoside
MBHA	Methylbenzhydrylamine Hydrochloride
MESNA	Sodium 2-sulfanylethanesulfonate
RFP	Red fluorescent protein
TAMRA	5 (and 6) – Carboxytetramethylrhodamine
Tris-Cl	Tris(hydroxymethyl)amino methane

APPENDIX II

ADDITIONAL FIGURE

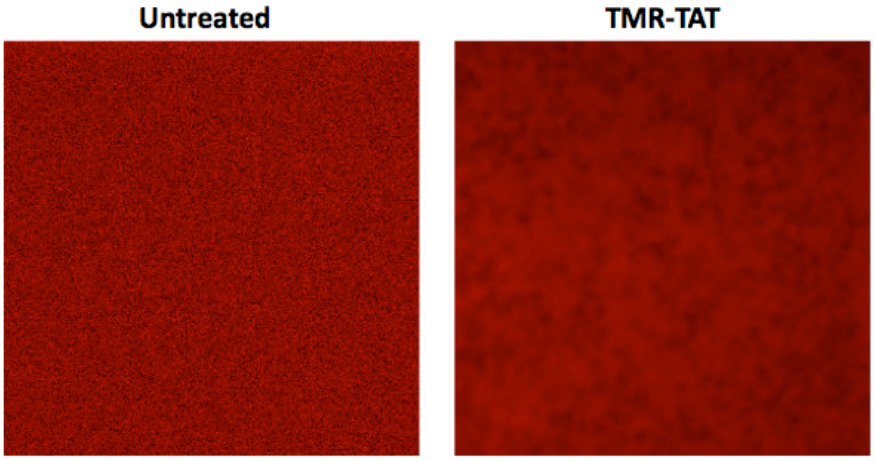

FIGURE A.1. **Background Fluorescence Comparison**. Dishes untreated with fluorescent CPP show random noise read as a fluorescent signal. Dishes treated with TMR-TAT or TMR-SS-TAT show speckling, presumably due to molecules adhering to the dish surface. Average pixel red intensity of untreated image is ~450 and of TMR-TAT is ~600.

CONTACT INFORMATION

Name:	Matthew Ellis Grunewald
Professional Address:	c/o Dr. Jean-Philippe Pellois Department of Biochemistry and Biophysics 103 Biochemistry/Biophysics Building Texas A&M University 2128 TAMU College Station, TX 77843
Education:	B.S., Biochemistry, Genetics, Texas A&M University, May 2012 Honors University Scholar Honors Research Fellows Goldwater Scholar Phi Beta Kappa